Towards an understanding of diffusion mechanism of bio-rejuvenators in aged asphalt binder through molecular dynamics simulation

Ding, Heyang; Wang, Hainian; Qu, Xin ; Varveri, Aikaterini; Gao, Junfeng ; You, Zhanping

DOI
10.1016/j.jclepro.2021.126927

Publication date
2021

Document Version
Final published version

Published in
Journal of Cleaner Production

Journal of Cleaner Production 299 (2021) 126927

Contents lists available at ScienceDirect

Journal of Cleaner Production

journal homepage: www.elsevier.com/locate/jclepro

Towards an understanding of diffusion mechanism of bio-rejuvenators in aged asphalt binder through molecular dynamics simulation

Heyang Ding [a], Hainian Wang [a, *], Xin Qu [a], Aikaterini Varveri [b], Junfeng Gao [a], Zhanping You [c]

[a] School of Highway, Chang'an University, 126 South Erhuan Middle Section, Xi'an City, Shaanxi Province, 710064, China
[b] Faculty of Civil Engineering & Geosciences, Delft University of Technology, Stevinweg 1, Delft, 2628 CN, Netherlands
[c] Department of Civil and Environmental Engineering, Michigan Technological University, 1400 Townsend Dr., Houghton, MI, 49931-1295, USA

ARTICLE INFO

Article history:
Received 2 December 2020
Received in revised form
23 March 2021
Accepted 27 March 2021
Available online 1 April 2021

Handling Editor: Zhen Leng

Keywords:
Diffusion mechanism
Microstructure morphology
Bio-rejuvenators
Aged asphalt binder
Molecular dynamics simulation

ABSTRACT

The use of reclaimed asphalt pavement (RAP) is a hot research topic in the field of road engineering, as there are still many issues to overcome so as to become standard engineering applications. The diffusion of virgin/aged asphalt binder is a key process to improve RAP performance. In this study, the asphalt binder diffusion models were developed by molecular dynamics (MD) simulation. Two kinds of bio-rejuvenators (BR-1 and BR-5) were chosen to represent the straight-chain and aromatic structures, respectively. The method of relative concentration, radial distribution function (RDF), and microstructure morphology were used to evaluate the effect of bio-rejuvenators on the diffusion process of virgin/aged asphalt binder. The results showed that bio-rejuvenators had a positive effect on the fusion process between virgin and aged asphalt binder. The volume diffusion coefficient based on asphalt binder diffusion models indicated that the bio-rejuvenators accelerated the fusion process between the virgin and asphalt binder. After adding bio-rejuvenators to the aged asphalt binder, the agglomeration intensity in the SARA fractions was reduced to different degrees. Due to the aging of asphalt binder, asphaltenes formed different types of micro-stacking phenomena such as "T-shaped stacking," "Face to Face stacking," and "Offset Face to Face stacking." The bio-rejuvenators of BR-1 and BR-5 exerted different regenerative effects during the diffusion process of aged asphalt binder. For BR-1, the "Pull-Out" and "Intercalation" effect can be observed in the process of asphaltene deagglomeration. "Pull-Out" is the main regenerative effect of BR-5 in aged asphalt binder. A strong electrostatic interaction occurs between BR-5 and PAHs in asphaltenes. Thus, BR-5 achieves the goal of aged asphalt binder regeneration by attracting PAHs.

1. Introduction

Road construction is an important foundation for urban infrastructure development. To meet increasingly significant sustainability challenges, numerous renewable materials have been gradually applied to road engineering (Ahmed and Dey, 2020). In recent years, bio-materials have attracted the attention of researchers due to their recyclability, environmental friendliness, high productivity, and low purchase price. They are obtained by a physical and chemical process using plant residues, animal manure, and waste food as raw materials. Bio-materials have important research significance for accelerating resource recycling and reducing carbon emission in industrial production (Ingrassia et al., 2020; Keykha and Asadi, 2017; Wang et al., 2020b).

Bio-oil, as a type of bio-material, is developed by the mature production process and is available commercially. Based on waste cooking (Gong et al., 2016), waste wood (Lei et al., 2018), sawdust (Gao et al., 2018a, 2018b), swine manure (Fini et al., 2011), algae (Chen et al., 2012; Du et al., 2011), and other materials, bio-oils have been gradually applied in the construction of asphalt binder pavements. As a possible alternative to petroleum asphalt binder, bio-modified asphalt binder is gradually becoming the focus of current research in the field of pavement materials. As a modifier of matrix asphalt binder, bio-oil can effectively improve the low-temperature performance of asphalt binder and reduce the occurrence of low-temperature cracking in pavements. Meanwhile, bio-

* Corresponding author.
E-mail address: wanghn@chd.edu.cn (H. Wang).

https://doi.org/10.1016/j.jclepro.2021.126927
0959-6526/

oil can play a synergistic and optimal role with other recyclable resources, such as waste rubber. Compared to conventional petroleum asphalt mixtures, bio-oil can significantly improve the fatigue resistance of asphalt mixtures and show good durability in service. Reclaimed asphalt pavement (RAP) has been getting considerable attention in road construction (Chen et al., 2019; Ge et al., 2019; Majidifard et al., 2019; Singh and Ransinchung, 2018). The goal of reducing greenhouse gas emissions and the consumption of non-renewable resources can be achieved by the application of RAP. As a rejuvenator for aged asphalt binder, it has been reported that the performance of pen-grade 40/50 grad aged asphalt binder after waste cooking oil regeneration is close to that of pen-grade 80/100 virgin asphalt binder (Asli et al., 2012; Zargar et al., 2012). Date seed oil can reduce the viscosity of aged asphalt binder. In addition, the regenerative effect of date seed oil can improve the fatigue life by 18–26% compared to aged asphalt binder (Mirhosseini et al., 2018). Bio-rejuvenator extracted from waste wood replenishes the lost light components in aged asphalt binder. It can also restore the rutting resistance of aged asphalt binder to a large extent. With the content of 15% and 20% bio-rejuvenator, the rutting resistance of the regenerated asphalt binder was very close to that of the virgin asphalt binder (Zhang et al., 2018).

Based on the aforementioned, some rheology and mechanical results have been obtained regarding the interaction between asphalt binder and bio-rejuvenators. The microscopic driving mechanisms of bio-rejuvenators to restore the performance of aged asphalt binder cannot be revealed through testing methods such as the rheology method (Behnood, 2019). It is also difficult to elucidate the regeneration mechanism at the atomic scale even by using microscopic detection methods in materials science, such as Atomic Force Microscopy (AFM), Scanning Electron Microscope (SEM), Transmission Electron Microscope (TEM), etc. In addition, the high financial cost limits the application of microscopic detection methods in bio-rejuvenators research.

Molecular dynamics (MD) is a virtual experimental method that is used to characterize the motion properties of a particle by solving the Newton motion equations (Feng et al., 2020; Long et al., 2021; Yao et al., 2019; You et al., 2020). MD can overcome the shortcomings of the aforementioned macroscopic experimental methods. MD simulations can also describe the interaction and evolution of different substances at the atomic scale, such as the interaction process of bio-rejuvenators/aged asphalt binder. The performance restoration effects of bio-rejuvenators can be fully elaborated on in mechanical or rheological tests. However, investigating the behavior properties of bio-rejuvenators at the atomic level is important for an effective rejuvenator materials' design.

It has been demonstrated that amide and nitrogenous molecules are the key components of bio-rejuvenators to exert regenerative effects. The chemical structures of the two active ingredients have been constructed by Farideh Pahlavan et al. (2019) and Masoumeh Mousavi et al. (2016). Based on MD simulations, Mullins (2010), Li et al. (Li and Greenfield, 2014), and Greenfield (2011) have carried out extensive research on the microstructure, component characterization, and simulation treatment of petroleum asphalt binder, providing a methodological basis for the bio-rejuvenator's modified aged asphalt binder. In two studies, Pahlavan et al., 2018, 2019 analyzed bio-rejuvenators' action mechanism in aged asphalt binder based on density functional theory. During the recovery process, bio-rejuvenators are bound to the polar sites of the asphaltene nanoaggregates first (which was called "Lock-and-Key"). Then, bio-rejuvenators are embedded in the asphaltene stacking systems (which was called "*Intercalation*"). They increased the molecular gap between the asphaltenes by interfering and oxidizing the aromatic cores of the asphaltene. Similarly, Zadshir et al. (Zadshir, Mehdi et al., 2018a,b; Zadshir, M. et al., 2018a,b) simulated the interaction between amide groups and asphaltene, which increased the stacking distance in asphaltene agglomerations based on the *Large-scale Atomic/Molecular Massively Parallel Simulator* (LAMMPS) computing platform.

During research on the microscopic mechanisms of bio-rejuvenators, asphaltene was considered for only the regeneration process instead of SARA fractions (Asphaltene, resin, saturate, and aromatic). And the interaction of the rejuvenator/asphaltene is not inconsistent with the real aging environment. Molecules with a strong polar structure in asphalt binder can also have a negative effect on bio-rejuvenators. In addition, the fusion rate between aged and virgin asphalt binder is an unavoidable issue in current bio-rejuvenators' applications. An effective rejuvenator should be able to accelerate the fusion process between aged and virgin asphalt binder, increasing the usage percent of aged asphalt binder. In the fusion process of aged and virgin asphalt binder, it is in line with the actual engineering situation to investigate the microscopic mechanism of bio-rejuvenators, including micro-morphological research and diffusion rate calculation. However, these issues have rarely been studied in previous research.

To fulfill the issue raised in the previous section, this research aims to investigate the microscopic regenerative mechanism of bio-rejuvenators from the perspective of micro-morphology and diffusion rate based on MD simulations.

- Based on the relative concentration, the influence of bio-rejuvenators in the fusion process of aged and virgin asphalt binder is quantified;
- Based on radial distribution function (RDF), the influence of bio-rejuvenators on SARA fractions in aged asphalt binder is quantified during the diffusion process;
- During the fusion of aged and virgin asphalt binder, the microscopic morphological evolution process of asphaltene is analyzed, and the microscopic mechanism of bio-rejuvenators is elaborated.

2. Simulation methodology

2.1. Molecular dynamics simulation

In this study, all the simulation calculations were completed in *Materials Studio 8.0*. Considering that the research object is mainly organic compounds, *Condensed-phase Optimized Molecular Potentials for Atomistic Simulation Studies* (COMPASS) and universal force fields are extremely appropriate for this research. The COMPASS force field can accurately describe the interaction parameters of metallic and non-metallic atoms. The goal of large-scale calculations of organic polymer systems can be realized by the COMPASS field. The universal forcefield can help to quickly optimize the chemical structure of molecules and complete the pre-processing of complex organic polymer systems. The two force fields are applied in both structure optimization and simulation calculations. The universal force field can improve the efficiency of structure optimization, while the COMPASS force field can maintain the accuracy of simulation calculation.

The initial asphalt binder system was randomly generated based on the Monte Carlo method. Thus, the total energy of the asphalt binder system is high and unstable. In the MD simulations, the conformation with the lowest potential energy is defined as the most stable conformation. The process of finding the most stable conformation is defined as energy minimization. The goal of energy minimization of the asphalt system can be achieved with the help of geometry optimization and annealing simulations. The difference is that geometry optimization is completed at a constant

temperature, while annealing simulations can achieve the goal of energy minimization in a dynamic temperature cycle. In this study, the simultaneous use of both energy optimization methods can better handle complex systems of organic polymers, such as asphalt binder.

In the geometry optimization, 10,000 energy iteration calculations were carried out for the asphalt binder system by using the smart algorithm at 298 K (1 atm). In the temperature range of 98 K–598 K, five energy cycles were implemented for the asphalt binder system which completed the geometry optimization.

2.2. Molecular structures of asphalt binder and bio-rejuvenators

Asphalt binder is susceptible to degradation by external factors such as ultraviolet rays, water, and pressure. From a microscopic point of view, the aging process of asphalt binder is reflected by the change of elements and chemical bonds in molecular structure. For aged asphalt, groups near the benzene and unsaturated bonds (e.g., double bonds, triple bonds, etc.) are more susceptible to oxidation caused by external factors. Fourier Transform Infrared (FTIR) analysis of aged asphalt in different aging statuses reveals that a greater number of S=O bonds or C=O bonds are present in the structure of the aged asphalt binder (Jing et al., 2019; Qu et al., 2018a,b), as shown in Fig. 1. The carbon (C) or sulfur (S) atoms are oxidized and formed C=O or S=O in Fig. 1. The presence of oxidation leads to the presence of more oxygen (O) and sulfur (S) atoms in the structure of the molecule.

It is impractical and unnecessary to complete accurately the characterization of the chemical structure about the fractions in asphalt binder (Rogel, 1995; Wang et al., 2020a). Actually, some representative molecular structures are selected to represent complex organic polymer systems in MD simulations. In this study, the representative molecular structure of each asphalt fraction was chosen from the research results of Li et al. (Li and Greenfield, 2014) and Martín et al. (Martín-Martínez et al., 2015), as shown in Fig. 2 (Virgin Part). Considering Clar's theory (Martín-Martínez et al., 2015), the number of π-sextets of PAHs was optimized in the asphaltene molecular structure. A more stable asphaltene molecular structure was obtained by changing the position of the branched-chain and benzene ring.

According to the aforementioned asphalt binder aging mechanism, the virgin and long-term aged asphalt binder were characterized separately, as shown in Fig. 2. The continuous oxidation reaction in the long-term aged asphalt binder is considered. More oxygen and sulfur atoms were added to the long-term aged asphalt compared to the virgin asphalt binder. It is noteworthy that the asphaltene structure proposed by Martín et al. (Martín-Martínez et al., 2015) was used as a representative molecule for the asphaltene fraction (Asp) in this study. Previous researchers have mainly used the asphaltene molecule structure of Li et al. (Li and Greenfield, 2014). Li's asphaltene models are feasible in simulation calculations. However, due to the high energy of the molecular system, it is difficult to be stable in real chemical reactions over a long period of time.

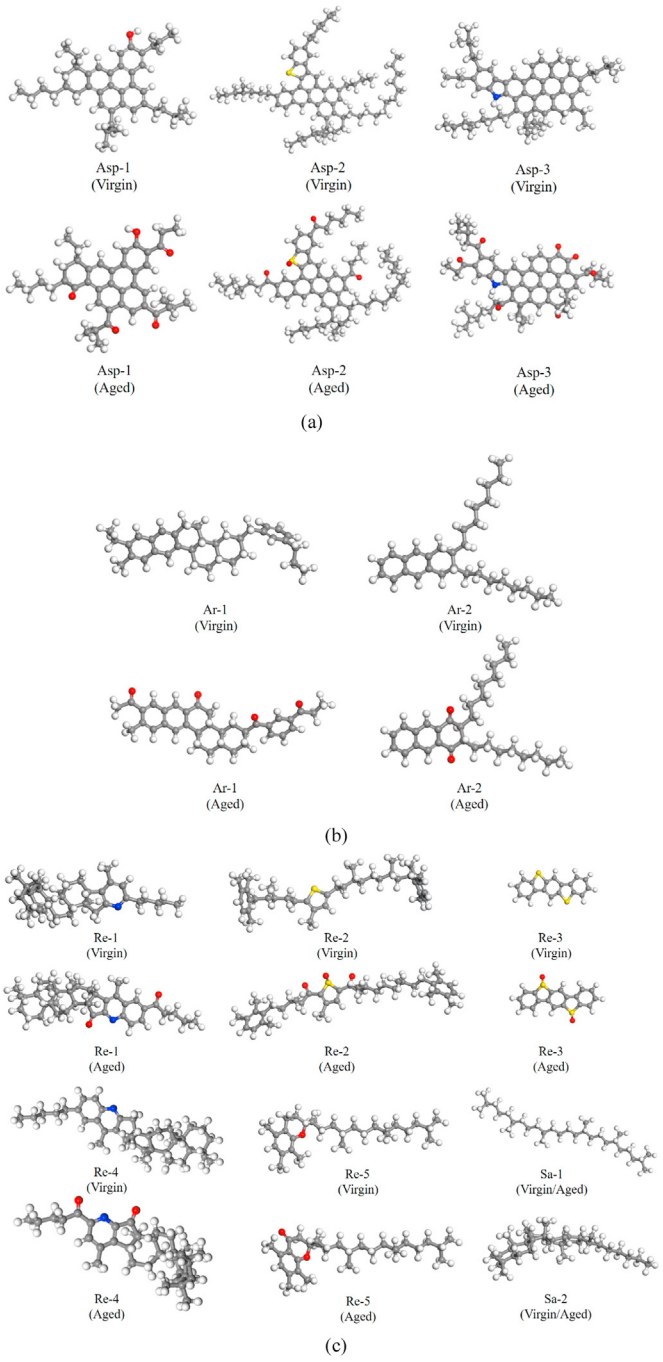

Fig. 2. The molecular structure of virgin and aged asphalt model: (a) asphaltene (Asp); (b) Aromatic (Ar); (c) Resin (Re) and Saturate (Sa). (Gray atoms: carbon atoms, yellow atoms: sulfur atoms, white atoms: hydrogen atoms, blue atoms: nitrogen atoms)(Li and Greenfield, 2014; Martín-Martínez et al., 2015).

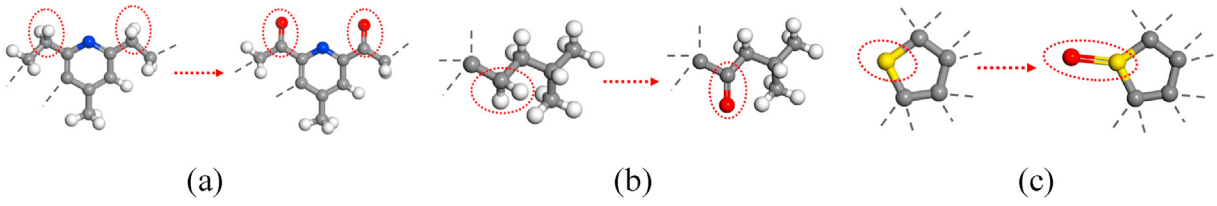

Fig. 1. The formation process of C=O and S=O under the environmental factors: (a) C=O (*Aromatic Heterocycles*); (b) C=O (*Straight Alkane*); (c) S=O (*Five-membered Heterocycles*).

Martín et al. (Martín-Martínez et al., 2015) optimized asphaltene models proposed by Greenfield et al. (Zhang and Greenfield, 2007a, b) and Li et al. (Li and Greenfield, 2014) according to the Clar sextet theory. These optimizations not only considered the branched-chain structure and the existing points but also analyzed the influence of the benzene number and position on the entire structural system. By comparing the difference of isomers, the most suitable asphaltene structure was screened out.

Rejuvenator is a substance that is chemical or biological-based and can rebalance the weight ratio of components in aged asphalt binder (Behnood, 2019). From the perspective of the molecular structure, Sun et al. (2016) analyzed the regenerating effect in aged asphalt binder based on its diffusion coefficient (which was calculated by the MSD curve) in the asphalt. Ding et al. (2016), Ahmed et al. (Ahmed and Hossain, 2020), and Xu et al. (2019) investigated the regenerating effect of different rejuvenators on aged asphalt binder. A true rejuvenator can both replenish the light fraction and reduce agglomeration by oxidative aging in the asphalt binder. Bio-rejuvenator is a kind of asphalt additive developed from bio-resources. Bio-rejuvenator extracted from swine manure can enhance the asphalt binder's rheological properties (Fini et al., 2011). With the addition of bio-rejuvenators extracted from waste cooking oil, the bio-asphalt mixtures are more highly ductile than conventional mixtures at a lower temperature (Wen et al., 2012).

Based on gas chromatography-mass spectrometry (GC-MS) and nuclear magnetic resonance (NMR) data analyses, bio-rejuvenator contained a large number of amide and nitrogenous functional groups (Fini et al., 2011; Xiu et al., 2012). Pahlavan et al., 2018, 2019 proposed the molecular structures (Number: BR-1~BR-7) of the main components in bio-rejuvenator. In terms of molecular structure form, these bio-rejuvenator molecules can be divided into straight chains and aromatic compounds. BR-1~BR-3 were the straight-chain structures, while BR-4~BR-7 were the aromatic structures. In order to make the research in this paper more comprehensive, two of the seven different representative molecular structures of bio-rejuvenators were selected, considering the differences in extraction sources and chemical structures of bio-rejuvenators (as shown in Fig. 3). Thus, two typical molecular structures (BR-1: C_{16} H_{33} N O, BR-5: C_8 H_7 N) were selected in this study, as shown in Fig. 3. The C_{16} H_{33} N O (BR-1) has the amide functional group and represents the straight chain structure, while the C_8 H_7 N (BR-5) has the nitrogen-containing functional group and represents the aromatic compounds structure.

2.3. The construction of asphalt binder models with bio-rejuvenators

In this study, in order to accurately characterize the chemical and physical structure, the modified 12-components molecular structure (Li and Greenfield, 2014; Martín-Martínez et al., 2015) was selected to construct the asphalt binder model. The detailed compositions of the virgin asphalt binder are listed in Table 1. For aged asphalt binder, oxidation affects the bonds and groups in the structure of the components. The number of ketone and sulfoxide function groups increased. Thus, this study referred to the characterization method of aged asphalt binder proposed by Xu et al. (2018) and Qu et al. (2018a,b), as shown in Table 2. The adopted aged asphalt model was artificially oxidized to achieve the chemical structural characteristics of real aged asphalt binder. Another feature that can characterize the phenomenon of asphalt binder aging is the change in the weight ratio of each fraction. The mass proportion of the saturated and aromatic fractions decrease, while the proportion of asphaltene increases by thermodynamic effect. This is because of the volatilization of the light fractions or their conversion into heavy fractions. Meanwhile, experimental studies have shown that saturate is the least sensitive to oxidative aging (Xu and Wang, 2017). It is rarely changed with the external environment and aging time due to the lack of polar atoms. Thus, with reference to the results of Qu et al. (2018a,b), the weight ratio of molecular components was adjusted in this research to reflect the degree of asphalt binder aging. The detailed compositions of the aged asphalt binder are listed in Table 3. The virgin asphalt model represents the fresh asphalt. The aged asphalt model represents the long-term aged asphalt. The virgin, aged, and aged asphalt binder with bio-rejuvenator models were optimized by annealing simulation and molecular dynamics calculation at 298 K.

2.4. The construction of asphalt binder diffusion models with bio-rejuvenators

An effective rejuvenator should have the ability to induce the movement of aging asphalt binder molecules and improve the mobility of the aging asphalt binder. From a microscopic point of view, the fusion of virgin and aged asphalt binder can be considered as an interfacial movement behavior (Sun and Wang, 2019). Different types of molecules migrate and stay continuously at the interface in virgin/aged asphalt binder. The diffusion process depends on environmentally relevant parameters (e.g. temperature,

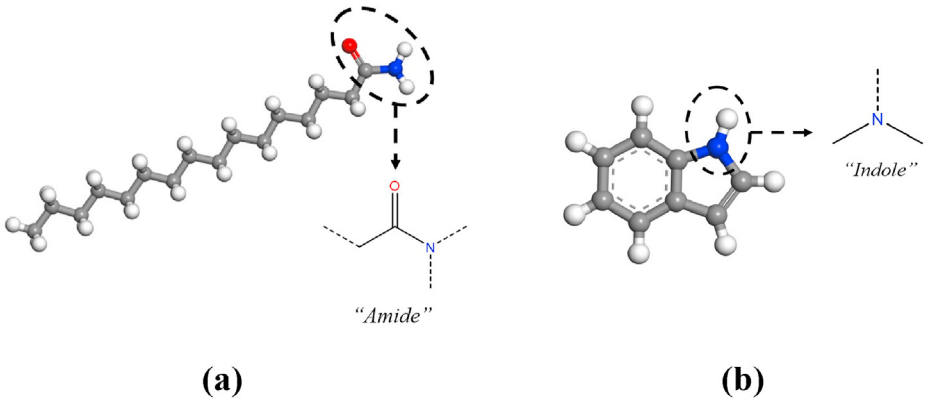

Fig. 3. Straight-chain and aromatic molecular structures: (a) C_{16} H_{33} N O (BR-1); (b) C_8 H_7 N (BR-5)(Pahlavan et al., 2019).

Table 1
The weight ratio of different fractions in virgin asphalt binder.

Fraction		Chemical formula	Molar mass (g/mol)	Weight (%)	Number in virgin asphalt model
Asphaltene	Asp-1	C_{42} H_{54} O	574.893	17.8	6
	Asp-2	C_{72} H_{98} S	995.636		4
	Asp-3	C_{66} H_{81} N	888.381		8
Saturate	Sa-1	C_{30} H_{62}	422.826	15.5	14
	Sa-2	C_{35} H_{62}	482.881		14
Aromatic	Ar-1	C_{35} H_{44}	464.737	41.4	36
	Ar-2	C_{30} H_{46}	406.698		42
Resin	Re-1	C_{40} H_{59} N	553.919	25.3	4
	Re-2	C_{40} H_{60} S	572.980		4
	Re-3	C_{18} H_{10} S_2	290.398		6
	Re-4	C_{36} H_{57} N	503.859		4
	Re-5	C_{29} H_{50} O	414.718		30

Table 2
The number of S═O and C═O in each structure.

Fraction	Structure	Virgin Asphalt Model		Aged Asphalt Model	
		C═O	S═O	C═O	S═O
Asphaltene	Asp-1	0	0	4	0
	Asp-2	0	0	3	1
	Asp-3	0	0	7	0
Saturate	Sa-1	0	0	0	0
	Sa-2	0	0	0	0
Aromatic	Ar-1	0	0	4	0
	Ar-2	0	0	2	0
Resin	Re-1	0	0	2	0
	Re-2	0	0	2	1
	Re-3	0	0	0	2
	Re-4	0	0	2	0
	Re-5	0	0	1	0

pressure, molecular morphology, molecular mass, etc.). The involvement of rejuvenators can increase the migration of molecules and accelerate the fusion of virgin/aged asphalt binder. In order to simulate the diffusion process on the MD computing platform, bi-diffusion models containing an artificial vacuum crack were constructed in this study. Modern atomic physics proves that atoms at an interface are not in close contact but have certain gaps between them. Therefore, in order to simulate the contact interface between two asphalt binders in a real environment, a vacuum crack with a thickness of 5 Å was set up. Furthermore, considering the periodic boundary conditions and directional diffusion, a 15 Å-length vacuum layer was set on one side of the asphalt binder, as shown in Fig. 4.

The different types of asphalt binder diffusion models are listed in Table 4. A virgin-virgin diffusion model and aged-aged diffusion model were used as the control group for this study, while a bio-aged-virgin diffusion model was used as the experimental group. Based on the *Amorphous Cell* module in the *Materials Studio* computing platform, the bio-rejuvenators with a content of 15% (weight ratio) (BR-1:BR-5 = 1:1) were added to the previous aged asphalt binder model. Exactly the same optimized and calculated treatment procedure was applied to the aged asphalt binder (containing BR-1 and BR-5).

After the geometry optimization, the dynamic calculation for 250 ps was applied to the diffusion models to allow the asphalt binder system to diffuse close freely in the *NVT* ensemble (453 K). The Nosé & Nosé-Hoover method was used to keep the temperature of the asphalt binder system stable during the diffusion process. The Nosé & Nosé-Hoover method can adjust both the velocity and the coordinates of the molecules. Thus, it is the closest temperature control method to the real diffusion process.

3. Model simulation reliability verification

3.1. Density (ρ) and glass transition temperature (T_g)

This anneal simulation procedure can ensure that the asphalt molecular system becomes more reasonable, as shown in Fig. 5 (a). The densities of the virgin, aged, and bio-aged asphalt binder models are shown in Fig. 5 (b). The densities of the models have reached a steady-state after a 50 ps simulation. In this study, all the results of molecular agglomeration and diffusion characterization were completed in a stable state. In 298 K and 1 atm, the stable densities of the virgin, aged, and bio-aged asphalt binder models were around 1.01 g/cm^3, 1.09 g/cm^3, and 1.06 g/cm^3, respectively (Cui et al., 2020; He et al., 2020; Qu et al., 2018a,b). The densities of these asphalt models obtained by molecular dynamic simulation were very close to the real measured value (Qu et al., 2018a,b; Read and Whiteoak, 2003; Sun et al., 2018; Sun and Wang, 2020).

The temperature of the asphalt binder system was gradually heated from 298 K to 598 K. The heating stage can help the asphalt

Table 3
The weight ratio of different fractions in aged asphalt binder.

Fraction		Chemical formula	Molar mass (g/mol)	Weight (%)	Number in aged asphalt model
Asphaltene	Asp-1	C_{42} H_{46} O_5	630.825	23.6	8
	Asp-2	C_{72} H_{92} O_4 S	1053.58		6
	Asp-3	C_{66} H_{67} N O_7	986.262		8
Saturate	Sa-1	C_{30} H_{62}	422.826	14.5	12
	Sa-2	C_{35} H_{62}	482.881		14
Aromatic	Ar-1	C_{35} H_{36} O_4	520.669	32.6	26
	Ar-2	C_{30} H_{42} O_2	434.664		30
Resin	Re-1	C_{40} H_{55} N O_2	581.885	29.3	4
	Re-2	C_{40} H_{56} O_3 S	616.945		4
	Re-3	C_{18} H_{10} O2 S_2	322.396		8
	Re-4	C_{36} H_{53} N O_2	531.825		4
	Re-5	C_{29} H_{48} O_2	428.701		34

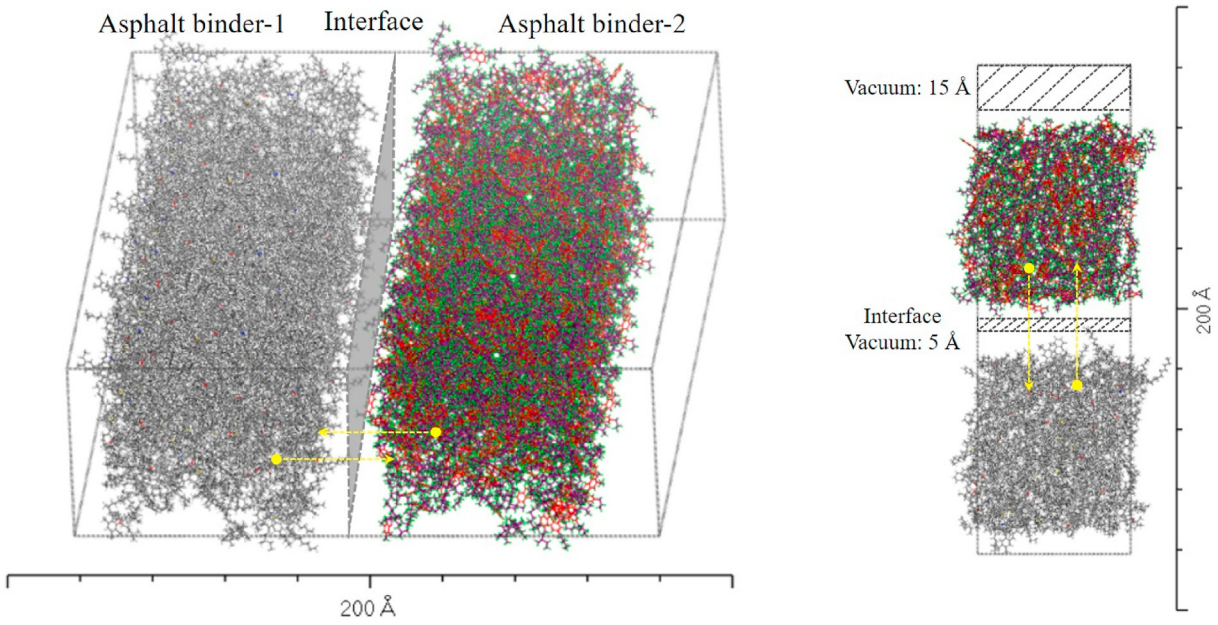

Fig. 4. The construction of asphalt model in different aging states: (a) diffusion model with a center crack; (b) vacuum layers in the diffusion model from cross sectional view.

Table 4
The different type of asphalt binder diffusion models.

Asphalt binder diffusion models (Shortened form)	Asphalt binder-1	Asphalt binder-2
Virgin-virgin diffusion model	Virgin asphalt binder	Virgin asphalt binder
Aged-aged diffusion model	Aged asphalt binder	Aged asphalt binder
Bio-aged-virgin diffusion model	Bio-aged asphalt binder (Aged asphalt binder contained BR-1 and BR-5)	Virgin asphalt binder

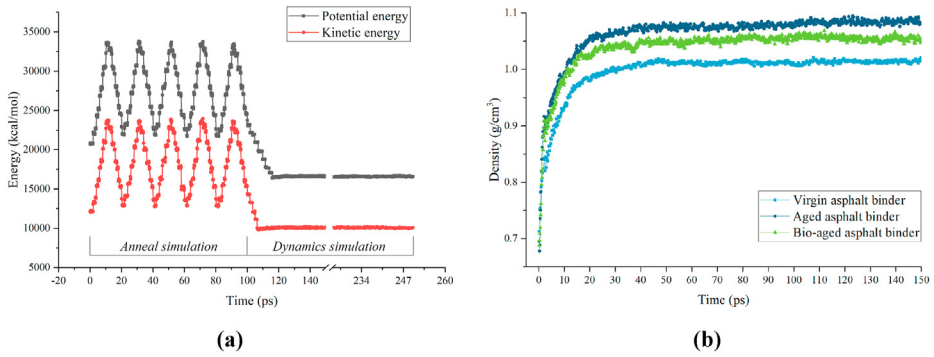

Fig. 5. Energy and density processes of asphalt models at different aging states: (a) energy variation in the Anneal simulation; (b) density variation in the dynamics simulation.

models to eliminate unreasonable molecular structure conformations to a certain extent. Then, the temperature was decreased from 598 to 98 K. The process of the cooling stage was used as the analysis for the glass transition temperature, as shown in Fig. 6.

According to thermodynamic theory, the relationship between the specific volume and temperature meets different linear relationships in different temperature regions. Between the high-temperature and low-temperature regions, there exists a *state transition zone* for asphalt. This state transition zone can be observed in the black dotted ellipse in Fig. 6. The temperature corresponding to the transition zone was called the glass transition temperature (T_g). The glass transition temperatures are 283.09 K and 267.06 K for virgin and aged asphalt binder, respectively. The glass transition temperature is 265.86 K for the bio-aged asphalt binder with BR-1 and BR-5. The results of this simulation are also similar to the simulations and experimental results of others (Broome, 1964; Sun and Wang, 2020; Zhu and Zhou, 2019).

3.2. Radial distribution function (RDF) and solubility parameter (δ)

The molecular dynamic calculation and anneal simulation (AS) made the asphalt system more stable. The radial distribution function (RDF) and solubility parameter (δ) analysis were calculated based on it. The RDF is an important method for analyzing the internal structure of organic polymer materials. The basic principle of the RDF is to solve for the appearance probability of other molecules around the reference molecule. Mathematically, the RDF is defined as the ratio between the local density of the reference molecule and the bulk density of the system. When the distance to the reference molecule is large enough, the local density is equal to

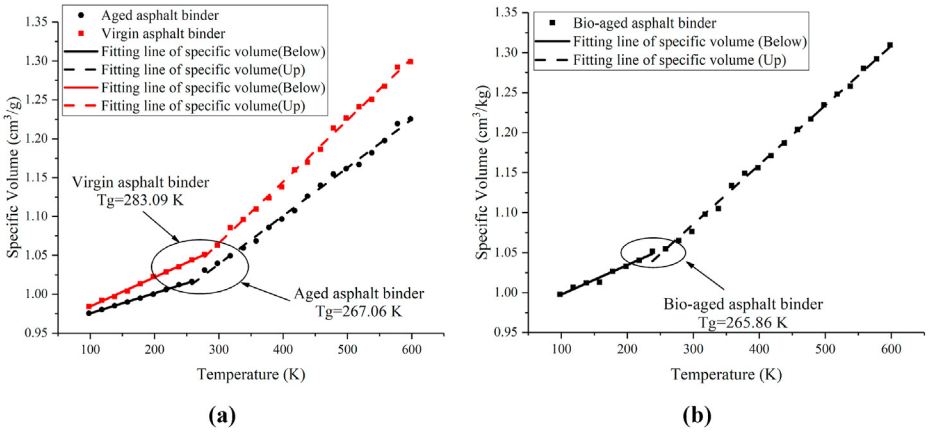

Fig. 6. The glass transition temperature of asphalt binder models: (a) virgin and aged asphalt binder model; (b) bio-aged asphalt binder model.

the bulk density, i.e., the RDF value is close to 1.

The mathematical expression of the RDF function is shown in Eq. (1). When in the same state, the RDF curve of the same type of chemical should be similar. The microscopic properties of asphalt binder can vary depending on the oil source, but its RDF curve should be similar. Unlike metals, asphalt binder is an amorphous substance. Thus, the structural features of asphalt binder should be long-range disordered and short-range ordered in the microscopic scale. Previous research results (Ding et al., 2015; Guo et al., 2020; Long et al., 2020; Su et al., 2020) have shown that the RDF of asphalt binder exhibits sharp oscillation peaks when r is in the range of 0–3 Å (Short-range). When r is in the range of 3–5 Å (Short-range), the amplitude of oscillation is not very obvious. After r exceeds 5 Å (Long-range), the RDF is smooth and tends to 1. This indicates that the particle distribution in the asphalt system is irregular.

$$g(r) = \frac{1}{4\pi r^2 \delta r \rho} \cdot \frac{\sum_{t=1}^{T} \sum_{j=1}^{N} \triangle N(r \rightarrow r + \delta r)}{N \times T} \tag{1}$$

where ρ is the average density of the molecular system; r is the distance from the reference molecule; N is the total number of molecules; $T$is total time calculated (steps); δr is distance difference; $\triangle N$is the number of molecules in the region between r and $r + dr$.

The RDF results of asphalt binder models in this research are shown in Fig. 7. It is shown that the g(r) all reached 1 at a distance of more than 5 Å. This indicates that the asphalt binder system in this research, in general, obeyed the basic structural properties of asphalt binder materials. For aged asphalt binder, the maximum value of the RDF reaches 10 when r is in the range of 0–3 Å. For virgin asphalt binder, the maximum value of the RDF reaches 8. This indicates that the molecular agglomeration in the interior of aged asphalt binder is more significant than that of the virgin. In addition, the number of peaks and the peaks in the 0–3 Å range in the aged asphalt binder is more than in the virgin. This is consistent with the research results of other scholars (Long et al., 2020; Xu and Wang, 2018).

The cohesive energy density (*CED*) characterizes the cohesive energy of a substance per unit cell volume. The *CED* can be used to calculate the solubility parameter (δ) of a substance, as shown in Eq. (2).

$$\delta = \sqrt{CED} = \sqrt{\frac{E_{coh}}{V}} \tag{2}$$

where *CED* is cohesive energy density; E_{coh} is the cohesive energy of a system of molecules; V is the space volume which is occupied by the molecule.

$$E_{coh} = -\langle E_{inter} \rangle = \langle E_{intra} \rangle - \langle E_{total} \rangle \tag{3}$$

where E_{inter} is the total energy between all molecules; E_{total} is the total energy of a system; E_{intra} is intra-molecular energy. The

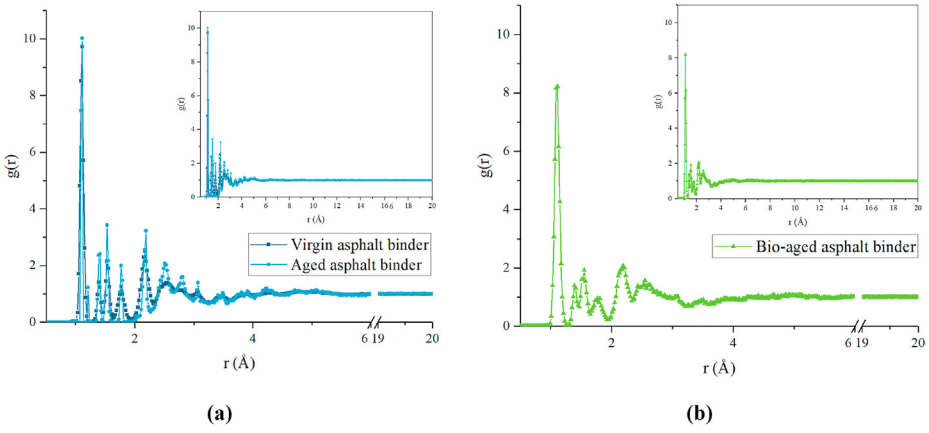

Fig. 7. The radial distribution function (*RDF*) of asphalt binder models: (a) virgin and aged asphalt binder; (b) bio-aged asphalt binder.

brackets $\langle \cdot \cdot \cdot \rangle$ represent an average over an *NPT* or *NVT* ensemble.

In the MD simulation, E_{coh} and V are obtained from the dynamics trajectory data extracted from the *NPT* ensemble. The solubility parameters of the asphalt binder are calculated based on Eq. (2) and (3). Table 5 shows that the solubility parameters of aged asphalt were significantly higher than that of virgin asphalt. This indicates that the cohesive energy density in aged asphalt was higher than that in virgin asphalt.

4. The recovery evaluation of bio-aged asphalt binder performance based on multiple micro-analytical methods

4.1. The evaluation method of relative concentration

Due to the free movement of the asphalt binder system, the local density was different in every position of the diffusion space. Relative concentration can make an accurate analysis of the density spatial distribution during the diffusion process. Relative concentration is an important function to characterize the density distribution of substances in a mixed molecular system. It is defined as the proportion of the local density to the bulk density. When the local space does not contain any atoms or molecules, the relative concentration should be 0. If the substance has sufficient diffusion in the constant space, the density at every position in this space should be the same as the average density of the system (Bulk density). The relative concentration and slab concentration of particles can be calculated according to Eq. (4) and (5). (Liu et al., 2020; Long et al., 2020).

$$RC_i = \frac{C_i}{C_{bulk}} \tag{4}$$

$$C_i = \frac{N_i}{V_i} \tag{5}$$

where RC_i is the relative concentration of the slab i; C_i is the concentration of the slab i; C_{bulk} is the bulk concentration; N_i is the number of particles in the slab i; V_i is the volume of the slab i.

Furthermore, the diffusion process of the asphalt system is a three-dimensional dynamic movement process. Previous literature (He et al., 2020) has proposed a self-healing rate (SH_{mic}) to quantitatively describe the self-healing behavior of asphalt binder. However, the proposed calculation method of self-healing rate is complicated and does not reflect the three-dimensional motion characteristics of the particles. The essence of the self-healing behavior of asphalt binder is consistent with the asphalt binder diffusion process in this study, i.e., the collision and movement of particles. Based on the concept of the self-healing rate, this study proposed to use the volume diffusion coefficient (C_d) to quantitatively describe the diffusion process of asphalt binder and the performance recovery effect of bio-rejuvenators. The introduced volume parameters were used to express the three-dimensional motion characteristics of the asphalt binder system. The volume diffusion coefficient can be calculated in Eq. (6) and (7).

$$\overline{L} = \frac{L_1 + L_2}{2} \tag{6}$$

$$C_d = \frac{\overline{L} \times S_d}{T} \tag{7}$$

where L_1 and L_2 are displacement (Å) of asphalt system on both sides; $\overline{L}$ is the average displacement of L_1 and L_2; S_d is the diffusion area of asphalt system; C_d is the volume diffusion coefficient of asphalt system; T is the diffusion time of asphalt system.

The fusion of a separated asphalt system is a very long process. After the consideration of the conflicts between the computing resource and simulation accuracy, the 250 ps of dynamic calculation (the *NVT* ensemble) was applied to the separated asphalt binder system. After sufficient diffusion of the asphalt binder system, the distribution of asphalt binder in the *OX*, *OY*, and *OZ* directions was analyzed by the relative concentration function. Fig. 8 showed the relative concentration profile of the asphalt diffusion in the *OX* and *OY* directions after the 250 ps diffusion time. Intuitively speaking, the relative concentration of the three diffusion models was around 1 along the *OX* or *OY* direction.

In order to more rigorously analyze the stationarity and dispersion of the relative concentration, a time series analysis was applied in this study. The time series data of the relative concentration were constructed by converting the original distance coordinates into time coordinates. Based on the econometric theory, partial autocorrelation function (PACF) can be used to analyze the stationarity and dispersion of time series data, as shown in Fig. 9. As the lag increased, the PACF gradually approached 0. This reflected that the time series data of relative concentration had good stationarity. For the asphalt diffusion model, it indicates that the diffusion of asphalt was uniform in the *OX* and *OY* directions.

The start (0 ps) and end (250 ps) of this diffusion process were selected as the object of relative concentration analysis in the *OZ* direction. The relative concentration analysis of virgin-virgin, aged-aged, and bio-aged-virgin asphalt binder diffusion models is shown in Fig. 10 and Fig. 11. The curve of relative concentration has the obvious separation profile at 0 ps. The vacuum layer of 5 Å thickness set initially can be observed at the distance of around 70 Å in Fig. 10 (a). After the molecular diffusion, the relative concentration curve of the asphalt binder system shifted significantly. The separated asphalt binder system on both sides moves to the middle space simultaneously. The relative concentration in the middle area increased from 0 to about 0.7. This showed that the separated asphalt binder system has completed a certain degree of fusion. During the same time, the diffusion velocity of aged-aged asphalt binder system was much slower than the virgin-virgin, as shown in Figs. 10 (a) and Fig. 11 (a). In the aged-aged asphalt diffusion model, the movement distance L_1 on the right side was 10 Å, while the movement distance L_2 on the left side was around 11 Å. The volume diffusion rate was 119.23 $Å^3$/ps (Table 6) with a decrease of about 27.18% compared with the virgin-virgin. With the bio-rejuvenators, the diffusion rate of asphalt system recovered to a certain extent, as

Table 5
Solubility parameter of asphalt binder models.

Model Type	Solubility Parameter $(J/cm^3)^{0.5}$	Reference	
		Simulation Result	Test Result
Virgin asphalt binder	18.00 ± 0.23	18.10 (Sun and Wang, 2019); 17.55 (He et al., 2020)	13.30–22.50 (Menozzi et al., 2015; Yang et al., 2015)
Aged asphalt binder	18.04 ± 0.10	18.61 (Sun and Wang, 2019)	
Bio-aged asphalt binder	18.25 ± 0.15	–	

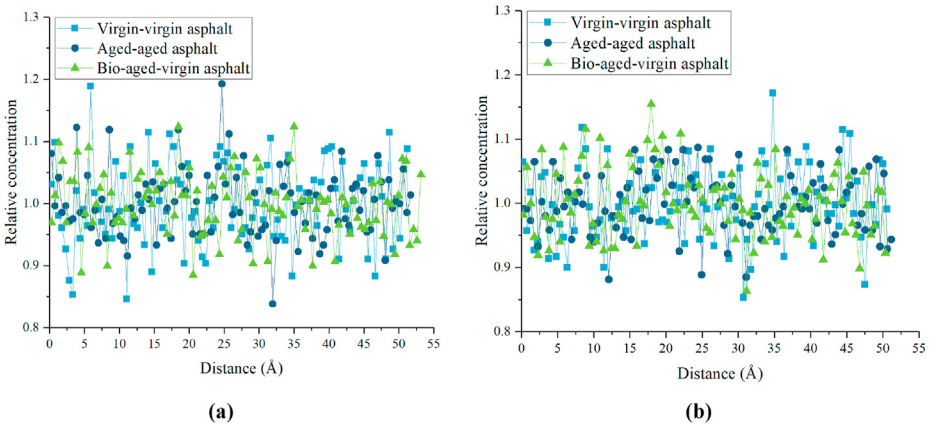

Fig. 8. The relative concentration of asphalt diffusion: (a) along the *OX* direction; (b) along the *OY* direction.

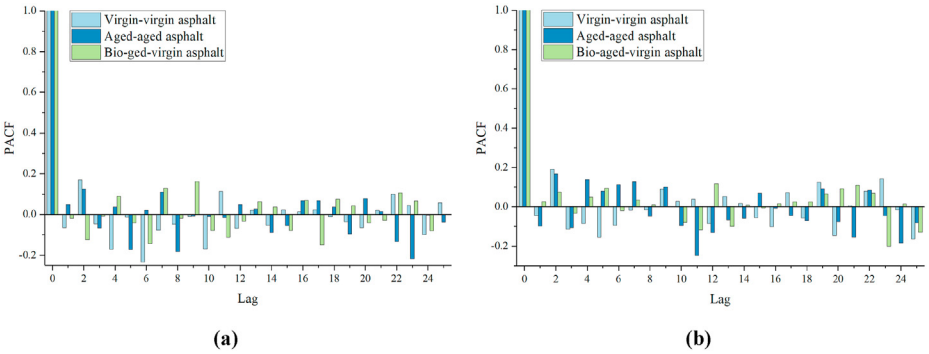

Fig. 9. The PACF analysis of asphalt diffusion: (a) along the *OX* direction; (b) along the *OX* and *OY* direction.

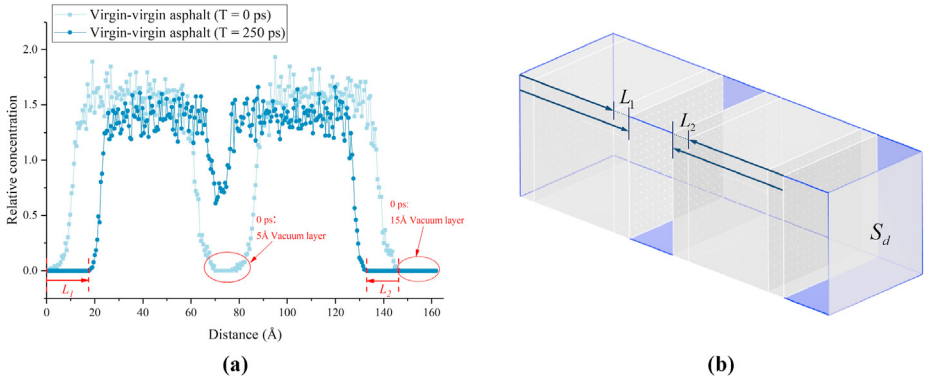

Fig. 10. The analysis and evaluation of asphalt diffusion model along the *OZ* direction: (a) relative concentration of virgin-virgin diffusion model; (b) principle of volume diffusion coefficient calculation.

shown in Fig. 11 (b). Compared with the virgin-virgin asphalt model, the volume diffusion rate of bio-aged-virgin asphalt diffusion model was 139.35 Å^3/ps, which was only reduced by about 14.89%. This shows that the bio-rejuvenators can effectively help aged asphalt binder to recover the diffusion performance and that they had a positive impact on the fusion process between virgin and aged asphalt binder.

4.2. The evaluation method of radial distribution function (RDF)

In order to further explain the role played by bio-rejuvenators, the microstructure of asphalt binder during the diffusion process was analyzed according to Eq. (1). Based on RDF curves, the effects of bio-rejuvenators on the internal structure of aged asphalt binder are demonstrated in this section. The RDF between asphaltene (Asp) and the other three fractions (Re, Sa, and Ar) are shown in Fig. 12.

The maximum peaks of Asp/Re, Asp/SA and Asp/Ar curves appear at 1.47 Å, 3.81 Å, and 4.25 Å, respectively. The agglomeration peaks of resin fraction (Asp/Re) in aged asphalt binder appeared first, followed by saturate (Asp/Sa) and aromatic (Asp/Ar) fractions. It is indicated that asphaltene was closest to resin, followed by saturate and aromatic in relative position. The maximum peak of Asp/Re curve was 12.044. In the range of 1–2 Å, multiple high peaks

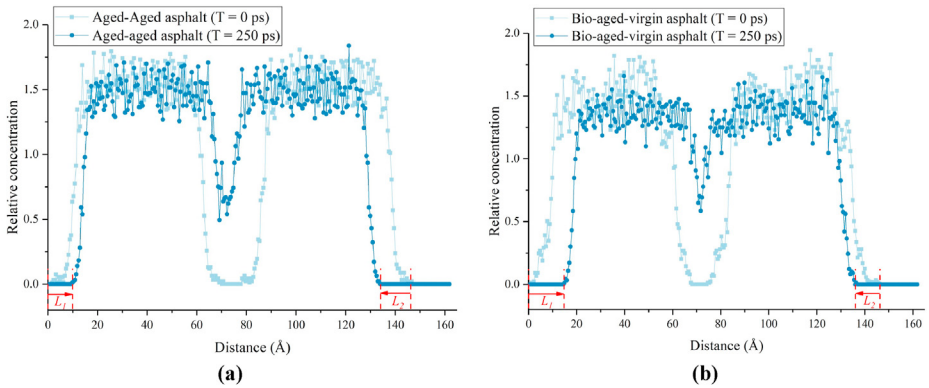

Fig. 11. The relative concentration analysis of asphalt diffusion model along the *OZ* direction: (a) aged-aged diffusion model; (b) bio-aged-virgin diffusion model.

Table 6
The volume diffusion coefficient of asphalt system diffusion process.

Asphalt binder diffusion models	Average displacement (Å)	Diffusion area (Å^2)	Volume diffusion coefficient (Å^3/ps)
Virgin-virgin	15.64	2617.32	163.74
Aged-aged	11.01	2707.32	119.23
Bio-aged-virgin	12.50	2786.96	139.35

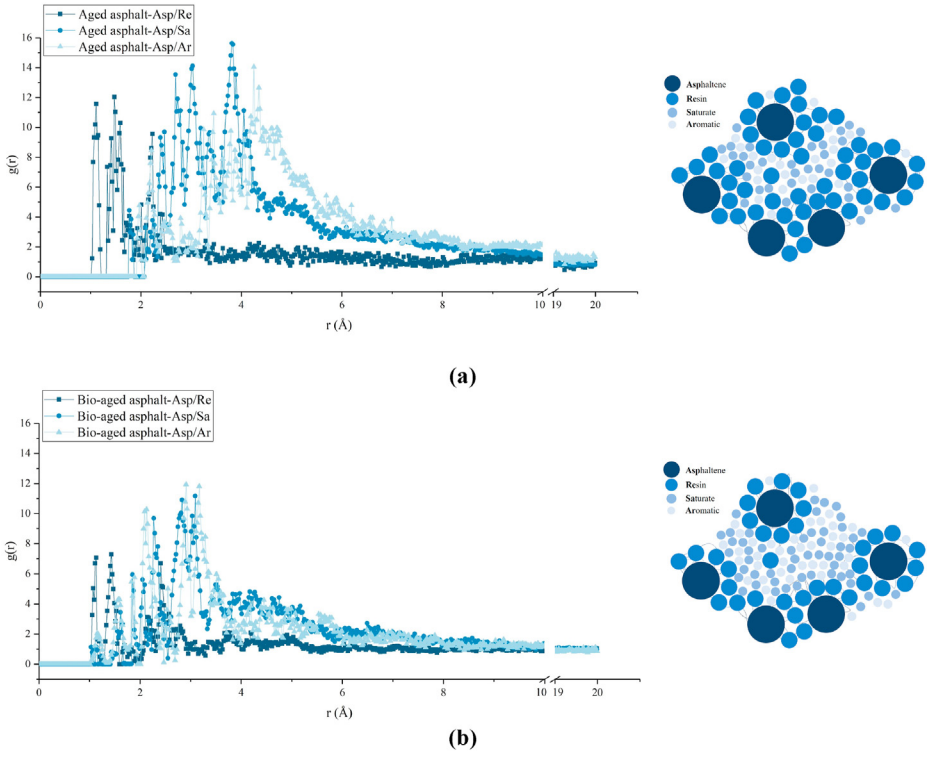

Fig. 12. The *RDF* of SARA-fractions: (a) aged asphalt binder; (b) bio-aged asphalt binder.

appeared in the Asp/Re curve. It is indicated that multiple adsorption layers of resin formed around the asphaltene, as shown in Fig. 12 (a) (Right side). The maximum peak of Asp/Sa and Asp/Ar was 3.81 and 4.25, respectively. Saturate fraction had multiple peak regions in its RDF curve, which extended from 2 to 4 Å. It is indicated that it has a wide distribution and local agglomeration in the aged asphalt system. Aromatic fraction also showed similar characteristics. In addition, there was an overlap in the distribution curves of the saturate and aromatic fractions, which is probably related to their molecular structure and molecular weight. The saturate and aromatic fractions are both in a viscous liquid state in 298 K, and there is some similarity in their molecular polarity (Huang et al., 2019). In brief, for aged asphalt binder, a large amount of resin is concentrated around the asphaltene and forms the asphaltene/resin agglomerations. Then, saturate and aromatic factions disperse around asphaltene/resin agglomerations.

After adding bio-rejuvenators to the aged asphalt binder, the inter-molecular RDF of the SARA fractions were analyzed, as shown

in Fig. 12 (b). The RDF curves in the bio-aged asphalt binder all migrated to different degrees in the presence of bio-rejuvenators. The maximum peaks of the Asp/Re, Asp/Sa, and Asp/Ar RDF curves appeared at 1.40 Å, 3.09 Å, and 2.91 Å, respectively. Compared with aged asphalt binder, the aggregation positions of resin, saturate, and aromatic fractions were all closer to asphaltene. Bio-rejuvenators changed the relative position relationship of fractions in asphalt binder. Referring to the theory of asphalt colloid structure, the bio-rejuvenators weakened the adsorption strength between resin and asphaltene and reduced the number of resin molecules surrounding asphaltene. As for saturate and aromatic, due to the reduction in the number of resin molecules, saturate and aromatic more easily filled the gaps in different asphaltene molecules. In the RDF curves, the peaks of saturate and aromatic curves were closer to the asphaltene. This dynamic process of microstructure can be seen in the schematic diagram of asphalt structure on the right side of Fig. 12. It is noteworthy that bio-rejuvenators play an active role in reducing nanoscale agglomerations. The bio-rejuvenators reduced the association that occurred in the different fractions, especially between the asphaltene and resin fraction. Compared to aged asphalt binder, the maximum peaks on the RDF curves of Asp/Re, Asp/Sa, and Asp/Ar were reduced by 40%, 29%, and 15%, respectively.

4.3. The evaluation method of microstructure morphology

To explain the regeneration mechanism of bio-rejuvenators in aging asphalt binder, micro-morphological analysis was applied to the MD simulations. Two kinds of bio-rejuvenators, BR-1 and BR-5, were analyzed for their effect on the morphology of asphaltene stacks. The aging process of asphalt binder materials can be reflected in the changes in the spatial distribution of asphaltene at the microscopic scale. In the aged asphalt binder, asphaltenes appeared "T-shaped stacking," "Face to Face stacking," "Offset Face to Face stacking," and other agglomeration phenomena. The polycyclic aromatic hydrocarbons (PAHs) structure is the material basis for the stacking of asphaltene. Due to the existence of the conjugated π-bond, the PAHs structures are strongly attracted to each other and the distance between the PAHs structures is shortened. External oxidation factors contributed to the presence of more S═O and C═O structures in the aged asphalt binder, which to some extent increases the intensity of asphaltene mutual attraction. This results in a greater stacking probability and a smaller stacking distance in the aged asphalt. The asphaltene stacking phenomenon can be observed generally in the aged asphalt binder model. In the "T-shaped stacking," the angle between the two asphaltenes was close to 90°. In the "Face to Face stacking" and "Offset Face to Face stacking," the distances of asphaltene centroid were 7.014 Å (Asp-2/Asp-3) and 5.466 Å (Asp-1/Asp-2), respectively, as shown in Fig. 13 (left side).

BR-1 showed the effect of "Intercalation" in the asphaltene stackings. The "Intercalation" effect of BR-1 was achieved by interfering with the π-π interaction between aromatic cores in the oxidized asphaltene. BR-1 caused the aromatic cores in the agglomerations to separate from each other to achieve the goal of increasing the internal gap distance. In Fig. 13 (a) (right side), BR-1 was embedded in the Asp-2/Asp-3 stack, increasing the gap between the two PAHs planes. The regenerative treatment model of "Intercalation" degraded the agglomeration of aged asphaltenes, and the distance between the centroids of Asp-2 and Asp-3 increased from 7.014 Å to 10.122 Å. BR-1 showed not only the "Intercalation" effect but also the "Pull-Out" effect. For "T-shaped stacking" in Fig. 13 (b) (right side), BR-1 showed the greater "Pull-Out" effect. When the amide group in BR-1 is in close position to the PAHs of the asphaltene (Asp-1) below, the violent repulsion causes the asphaltene (Asp-1) below to be pushed out of "T-shaped stacking." After the "Pull-Out" regeneration process of BR-1, their centroids were clearly not in the same vertical plane. It is indicated that BR-1 had a significant effect on the restricting of asphaltene agglomeration. Because of its straight chain structure and amide functional group, BR-1 can exert the "Pull-Out" and "Intercalation" effect simultaneously in the process of asphaltene deagglomeration.

The BR-5 molecules showed the effect of "Pull-Out," as showed in Fig. 13 (c) (right side). "Pull-Out" is a special regeneration effect which has not been mentioned in previous literature. The essence of "Pull-Out" effect is aromatic cores interaction. The electrostatic interaction can appear between BR-5 and PAHs because of the benzene ring plane. For "T" shape stacking asphaltene agglomeration, BR-5 can cause one asphaltene to shift and twist, disintegrating the entire "T-shaped stacking." More information about the "Pull-Out" effect of BR-5 is shown in Fig. 14. The presence of BR-5 caused the asphaltene (Asp-2) below to shift and twist in the dimer asphaltene in Fig. 14 (a). The original "T-shaped" space morphology was changed by BR-5, and the centroid distance of the two asphaltenes (Asp-1/Asp-2) was 10.239 Å. For the "Face to Face stacking," BR-5 can also increase the void distance inside the asphaltene stacking, as shown in Fig. 14 (b). The centroid distance of the two asphaltenes (Asp-1/Asp-3) was 9.470 Å. It was higher than the stacking distance of dimers in aged asphalt binder. It was shown that in different types of oxidized asphaltene agglomerations, BR-5 can still exert a positive regeneration effect.

The asphaltene nanoscale agglomerations can be obviously observed in the simulation environment. From the simulation results, it can be found that the regenerative mechanism exerted by the two bio-rejuvenators was obviously different. It may be related to their structural differences. BR-1 had a straight chain structure, while BR-5 had a benzene ring planar structure in Fig. 3. BR-1 can insert well into the asphaltene stack voids due to its straight chain-like structure. In Fig. 15, BR-1 and BR-5 decomposed the trimer asphaltene that existed generally in aged asphalt binder. In the trimer asphaltene of Asp-1~Asp-3, BR-1 molecular inserted into their central voids. It broke the spatial configuration of the original triple stacking with the aid of the BR-5 molecule. The BR-5 molecular had the same conjugated π-bond as the three asphaltene structures (Asp-1, Asp-2, and Asp-3).

5. Conclusions

This study demonstrated that MD simulation can help investigate the agglomeration and diffusion phenomena of asphalt binder systems. The reliability of the asphalt binder model was verified by density, glass transition temperature, RDF, and solubility parameters. The asphalt binder diffusion models were developed to investigate the effect of bio-regenerators (BR-1 and BR-5) on the diffusion process. The volume diffusion coefficient was proposed to quantitatively describe the diffusion process of asphalt binder. The relative position relation of the internal fractions (SARA) was analyzed based on the RDF results. Micro-morphological analysis was used for in-depth analysis and comparison of the recovery effects exerted by the two kinds of bio-regenerators. The main conclusions are as follows:

- After MD calculation and annealing simulation, the reliability of the asphalt binder models was verified by multiple indicators. The densities of asphalt binder models all reached a steady state after 50 ps. The density of aged asphalt binder was higher than that of virgin. The density of bio-aged asphalt binder is between virgin and aged asphalt binder. The glass transition temperatures were 283.09 K and

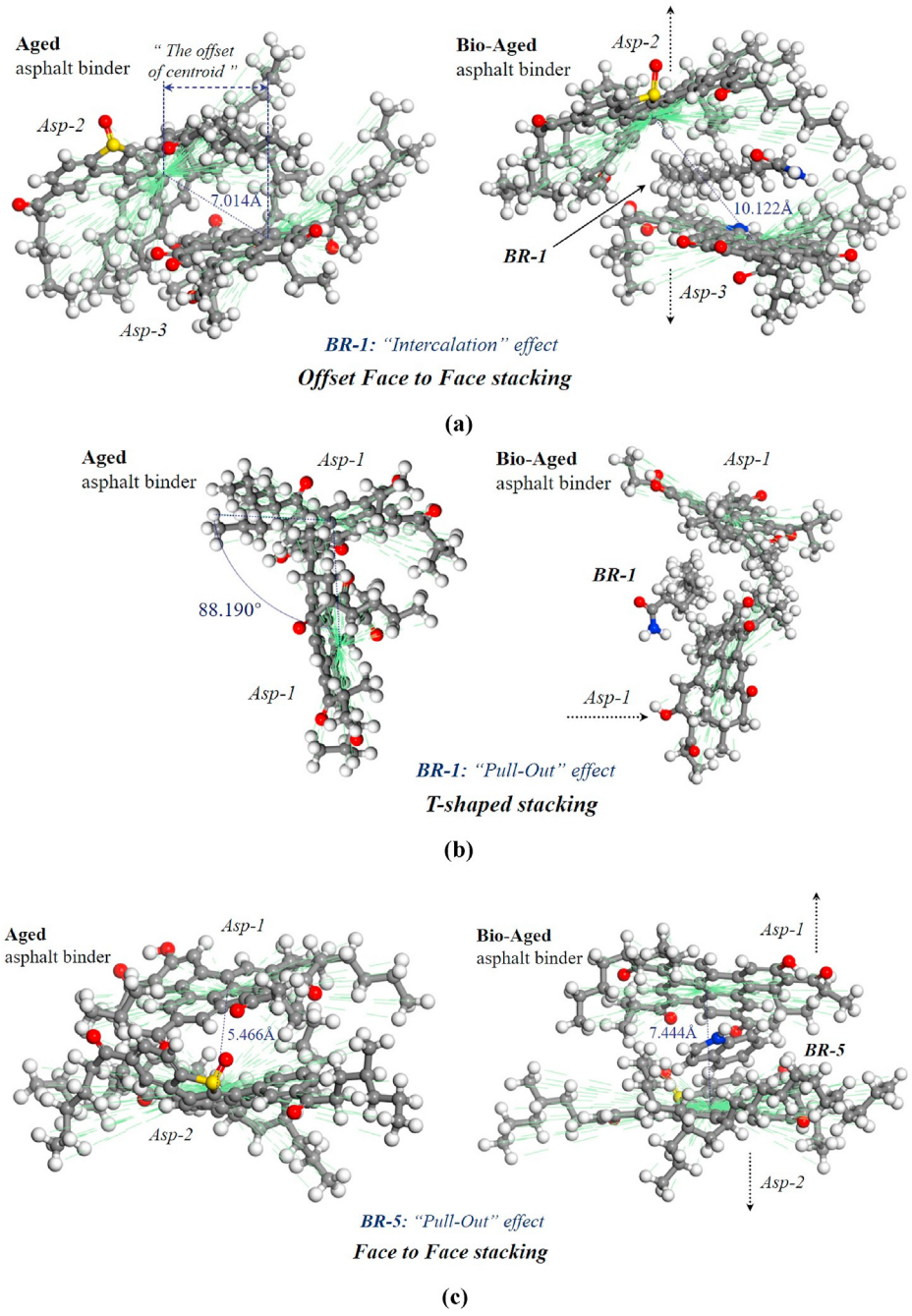

Fig. 13. The asphaltene agglomeration phenomenon in aged asphalt binder and regenerative effect of bio-rejuvenators: (a) "Intercalation" effect of BR-1 & in "Offset Face to Face stacking"; (b) "Pull-Out" effect of BR-1 in "T-shaped stacking"; (c) "Pull-Out" effect of BR-5 in "Face to Face stacking."

267.06 K for virgin and aged asphalt binder. The glass transition temperature of bio-aged asphalt binder was 265.86 K. The solubility parameter of virgin asphalt binder models was around 18.00 $(J/cm^3)^{0.5}$. The solubility parameters of aged and bio-aged asphalt binder were 18.04 and 18.25 $(J/cm^3)^{0.5}$, higher than that of virgin.

- Compared with the virgin-virgin asphalt binder diffusion model, the volume diffusion coefficient of aged-aged and bio-aged-aged was 119.23 $Å^3$/ps and 139.35 $Å^3$/ps, respectively. Aging of asphalt binder led to a decrease in diffusion efficiency of about 27.18% in the same diffusion time, whereas the diffusion efficiency of the bio-aged asphalt binder decreased by only 14.89%. Bio-rejuvenators can effectively help aged asphalt binder to recover diffusion performance, and they have a positive impact on the fusion process between virgin and aged asphalt binder.
- Based on RDF curves, the effects of bio-rejuvenators on the internal structure of aged asphalt binder were demonstrated. The agglomeration RDF peaks of resin fraction (Asp/Re) in aged asphalt binder appeared first, followed by saturate (Asp/Sa) and aromatic (Asp/Ar) fractions. After adding bio-rejuvenators to aged asphalt binder, the inter-molecular RDF of the SARA fractions in the bio-aged asphalt binder all migrated to different degrees in the presence of bio-

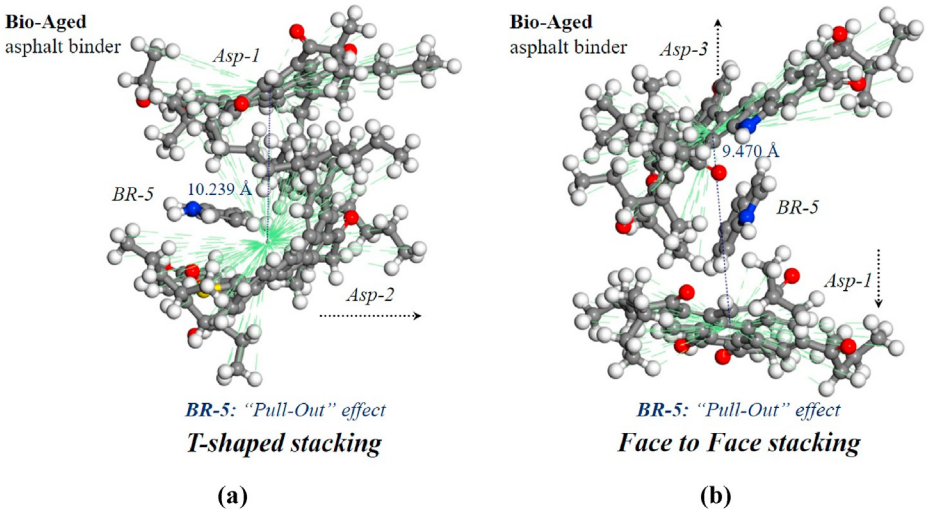

Fig. 14. The "Pull-Out" effect of BR-5 in asphaltene stacking: (a) BR-5 in "T-shaped stacking"; (b) BR-5 in "Face to Face stacking".

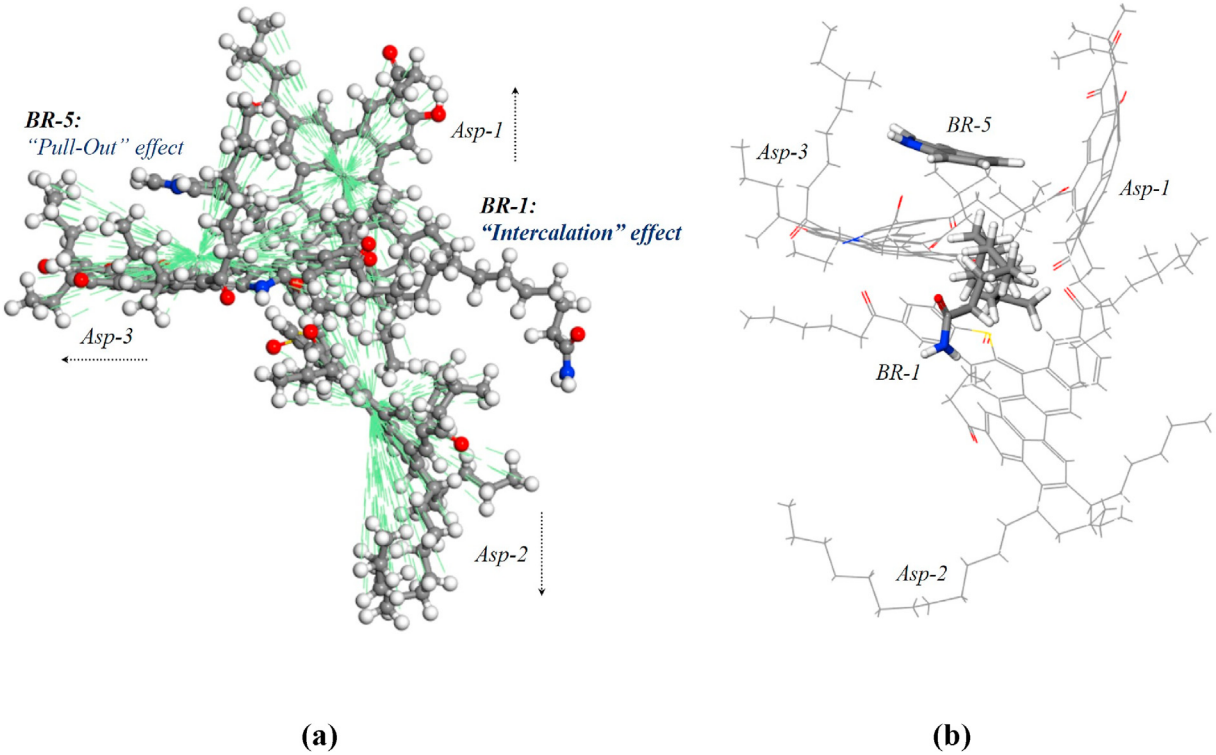

Fig. 15. Triple stacking of asphaltene agglomeration (Asp-1~Asp-3): (a) Ball-and-stick model; (b) Line/Ball-and-stick model.

rejuvenators. Compared to aged asphalt binder, the RDF maximum peaks of Asp/Re, Asp/Sa, and Asp/Ar were reduced by 40%, 29%, and 15%, respectively in bio-aged asphalt binder. Bio-rejuvenators played an active role in reducing nanoscale agglomerations.

- In the aged asphalt binder, asphaltene appeared as "T-shaped stacking," "Face to Face stacking," "Offset Face to Face stacking," and other agglomeration phenomena. The PAHs structure is the material basis for the stacking of asphaltenes. Due to the existence of the conjugated π-bond, the PAHs structures are strongly attracted to each other, and the distance between the PAHs structures is shortened. BR-1 has a straight chain structure and amide functional group. Thus, it can exert the "Pull-Out" and "Intercalation" effect simultaneously in the process of asphaltene deagglomeration. The BR-5 molecules showed the effect of "Pull-Out." The essence of the "Pull-Out" effect, which has not been mentioned in previous literature, is aromatic cores interaction. The electrostatic interaction can appear between BR-5 and PAHs because of the benzene ring plane.

CRediT authorship contribution statement

Heyang Ding: Conceptualization, Methodology, Validation, Investigation, Formal analysis, Writing – original draft. **Hainian Wang:** Supervision, Writing – review & editing, Project administration, Funding acquisition. **Xin Qu:** Supervision, Formal analysis, Writing – review & editing, Project administration, Funding acquisition. **Aikaterini Varveri:** Writing – review & editing. **Junfeng Gao:** Methodology, Writing – review & editing. **Zhanping You:** Software, Resources, Writing – review & editing.

Declaration of competing interest

The authors declare that they have no known competing financial interests or personal relationships that could have appeared to influence the work reported in this paper.

Acknowledgements

The work described in this paper is supported by the National Natural Science Foundation of China (No. 51878063, No. 52078048 and No. 52008029), the Fundamental Research Foundation of the Cornell University (No. 3001 0221 8718), and Postgraduate Research and Practice Program of Chang'an University (No. 300103703001, *The design optimization and noise reduction of elastic chip-seal based on aggregate micro-morphology characteristics*.).

Thanks are due to Ponan Feng (Chang'an University) for valuable discussion.

References

Ahmed, R.B., Hossain, K., 2020. Waste cooking oil as an asphalt rejuvenator: a state-of-the-art review. Construct. Build. Mater. 230, 116985.
Ahmed, S., Dey, K., 2020. Resilience modeling concepts in transportation systems: a comprehensive review based on mode, and modeling techniques. J Infrastruct. Preserv. Resil. 1 (1), 8–28.
Asli, H., Ahmadinia, E., Zargar, M., Karim, M.R., 2012. Investigation on physical properties of waste cooking oil – rejuvenated bitumen binder. Construct. Build. Mater. 37, 398–405.
Behnood, A., 2019. Application of rejuvenators to improve the rheological and mechanical properties of asphalt binders and mixtures: a review. J. Clean. Prod. 231, 171–182.
Broome, D.C., 1964. Asphalt: science and Technology. Nature 202 (4934), 739–740.
Chen, S., Gong, F., You, Z., Sousa, J.B., Ge, D., 2019. Development of a new asphalt mixture containing reacted and activated rubber and reclaimed asphalt pavement via superpave mix design and marshall mix design. In: Transportation Research Board 98th Annual Meeting. Washington DC, United States.
Chen, Y., Wu, Y., Zhang, P., Hua, D., Yang, M., Li, C., Chen, Z., Liu, J., 2012. Direct liquefaction of Dunaliella tertiolecta for bio-oil in sub/supercritical ethanol–-water. Bioresour. Technol. 124, 190–198.
Cui, B., Gu, X., Hu, D., Dong, Q., 2020. A multiphysics evaluation of the rejuvenator effects on aged asphalt using molecular dynamics simulations. J. Clean. Prod. 259, 120629.
Ding, Y., Huang, B., Shu, X., Zhang, Y., Woods, M.E., 2016. Use of molecular dynamics to investigate diffusion between virgin and aged asphalt binders. Fuel 174, 267–273.
Ding, Y., Tang, B., Zhang, Y., Wei, J., Cao, X., 2015. Molecular dynamics simulation to investigate the influence of SBS on molecular agglomeration behavior of asphalt. J. Mater. Civ. Eng. 27 (8), C4014004.
Du, Z., Li, Y., Wang, X., Wan, Y., Chen, Q., Wang, C., Lin, X., Liu, Y., Chen, P., Ruan, R., 2011. Microwave-assisted pyrolysis of microalgae for biofuel production. Bioresour. Technol. 102 (7), 4890–4896.
Feng, P., Wang, H., Ding, H., Xiao, J., Hassan, M., 2020. Effects of surface texture and its mineral composition on interfacial behavior between asphalt binder and coarse aggregate. Construct. Build. Mater. 262, 120869.
Fini, E.H., Kalberer, E.W., Shahbazi, A., Basti, M., You, Z., Ozer, H., Aurangzeb, Q., 2011. Chemical characterization of biobinder from swine manure: sustainable modifier for asphalt binder. J. Mater. Civ. Eng. 23 (11), 1506–1513.
Gao, J., Wang, H., You, Z., Mohd Hasan, M.R., 2018a. Research on properties of bio-asphalt binders based on time and frequency sweep test. Construct. Build. Mater. 160, 786–793.
Gao, J., Wang, H., You, Z., Yang, X., 2018b. Gray relational entropy analysis of high temperature performance of bio-asphalt binder, its mixture. Int. J. Pavement Res. Technol. 11 (7), 699–708.
Ge, D., You, Z., Chen, S., Liu, C., Gao, J., Lv, S., 2019. The performance of asphalt binder with trichloroethylene: improving the efficiency of using reclaimed asphalt pavement. J. Clean. Prod. 232, 205–212.
Gong, M., Yang, J., Zhang, J., Zhu, H., Tong, T., 2016. Physical–chemical properties of aged asphalt rejuvenated by bio-oil derived from biodiesel residue. Construct. Build. Mater. 105, 35–45.
Greenfield, M.L., 2011. Molecular modelling and simulation of asphaltenes and bituminous materials. Int. J. Pavement Eng. 12 (4), 325–341.
Guo, F., Zhang, J., Pei, J., Zhou, B., Falchetto, A.C., Hu, Z., 2020. Investigating the interaction behavior between asphalt binder and rubber in rubber asphalt by molecular dynamics simulation. Construct. Build. Mater. 252, 118956.
He, L., Li, G., Lv, S., Gao, J., Kowalski, K.J., Valentin, J., Alexiadis, A., 2020. Self-healing behavior of asphalt system based on molecular dynamics simulation. Construct. Build. Mater. 254, 119225.
Huang, M., Zhang, H., Gao, Y., Wang, L., 2019. Study of diffusion characteristics of asphalt–aggregate interface with molecular dynamics simulation. Int. J. Pavement Eng. 1–12.
Ingrassia, L.P., Lu, X., Ferrotti, G., Canestrari, F., 2020. Chemical, morphological and rheological characterization of bitumen partially replaced with wood bio-oil: towards more sustainable materials in road pavements. J. Traffic Transp. Eng. (Engl. Ed.) 7 (2), 192–204.
Jing, R., Varveri, A., Liu, X., Scarpas, A., Erkens, S., 2019. Ageing effect on chemo-mechanics of bitumen. Road Mater. Pavement Des. 1–16.
Keykha, H.A., Asadi, A., 2017. Solar powered electro-bio-stabilization of soil with ammonium pollution prevention system. Adv. Civ. Eng. Mater. 6 (1), 360–371.
Lei, Y., Wang, H., Chen, X., Yang, X., You, Z., Dong, S., Gao, J., 2018. Shear property, high-temperature rheological performance and low-temperature flexibility of asphalt mastics modified with bio-oil. Construct. Build. Mater. 174, 30–37.
Li, D.D., Greenfield, M.L., 2014. Chemical compositions of improved model asphalt systems for molecular simulations. Fuel 115, 347–356.
Liu, J., Yu, B., Hong, Q., 2020. Molecular dynamics simulation of distribution and adhesion of asphalt components on steel slag. Construct. Build. Mater. 255.
Long, Z., You, L., Tang, X., Ma, W., Ding, Y., Xu, F., 2020. Analysis of interfacial adhesion properties of nano-silica modified asphalt mixtures using molecular dynamics simulation. Construct. Build. Mater. 255, 119354.
Long, Z., Zhou, S., Jiang, S., Ma, W., Ding, Y., You, L., Tang, X., Xu, F., 2021. Revealing compatibility mechanism of nanosilica in asphalt through molecular dynamics simulation. J. Mol. Model. 27 (3), 81.
Majidifard, H., Tabatabaee, N., Buttlar, W., 2019. Investigating short-term and long-term binder performance of high-RAP mixtures containing waste cooking oil. J. Traffic Transp. Eng. (Engl. Ed.) 6 (4), 396–406.
Martín-Martínez, F.J., Fini, E.H., Buehler, M.J., 2015. Molecular asphaltene models based on Clar sextet theory. RSC Adv. 5 (1), 753–759.
Menozzi, A., Garcia, A., Partl, M.N., Tebaldi, G., Schuetz, P., 2015. Induction healing of fatigue damage in asphalt test samples. Construct. Build. Mater. 74, 162–168.
Mirhosseini, A.F., Kavussi, A., Tahami, S.A., Dessouky, S., 2018. Characterizing temperature performance of bio-modified binders containing RAP binder. J. Mater. Civ. Eng. 30 (8), 04018176.
Mousavi, M., Pahlavan, F., Oldham, D., Abdollahi, T., Fini, E.H., 2016. Alteration of intermolecular interactions between units of asphaltene dimers exposed to an amide-enriched modifier. RSC Adv. 6 (58), 53477–53492.
Mullins, O.C., 2010. The modified yen model. Energy Fuels 24 (4), 2179–2207.
Pahlavan, F., Mousavi, M., Hung, A.M., Fini, E.H., 2018. Characterization of oxidized asphaltenes and the restorative effect of a bio-modifier. Fuel 212, 593–604.
Pahlavan, F., Samieadel, A., Deng, S.G., Fini, E., 2019. Exploiting synergistic effects of intermolecular interactions to synthesize hybrid rejuvenators to revitalize aged asphalt. ACS Sustain. Chem. Eng. 7 (18), 15514–15525.
Qu, X., Liu, Q., Guo, M., Wang, D., Oeser, M., 2018a. Study on the effect of aging on physical properties of asphalt binder from a microscale perspective. Construct. Build. Mater. 187, 718–729.
Qu, X., Wang, D.W., Hou, Y., Oeser, M., Wang, L.B., 2018b. Influence of paraffin on the microproperties of asphalt binder using MD simulation. J. Mater. Civ. Eng. 30 (8), 04018191.
Read, J., Whiteoak, D., 2003. The Shell Bitumen Handbook, fifth ed. ed.
Rogel, E., 1995. Studies on asphaltene aggregation via computational chemistry. Colloids Surf. A Physicochem. Eng. Asp. 104 (1), 85–93.
Singh, S., Ransinchung, G.D., 2018. Durability properties of pavement quality concrete containing fine RAP. Adv. Civ. Eng. Mater. 7 (1), 271–290.
Su, M., Si, C., Zhang, Z., Zhang, H., 2020. Molecular dynamics study on influence of Nano-ZnO/SBS on physical properties and molecular structure of asphalt binder. Fuel 263, 116777.
Sun, D., Lin, T., Zhu, X., Tian, Y., Liu, F., 2016. Indices for self-healing performance assessments based on molecular dynamics simulation of asphalt binders. Comput. Mater. Sci. 114, 86–93.
Sun, D., Sun, G., Zhu, X., Ye, F., Xu, J., 2018. Intrinsic temperature sensitive self-healing character of asphalt binders based on molecular dynamics simulations. Fuel 211, 609–620.
Sun, W., Wang, H., 2019. Molecular dynamics simulation of diffusion coefficients between different types of rejuvenator and aged asphalt binder. Int. J. Pavement Eng. 1–11.
Sun, W., Wang, H., 2020. Self-healing of asphalt binder with cohesive failure: insights from molecular dynamics simulation. Construct. Build. Mater. 262, 120538.
Wang, H., Ding, H., Feng, P., Shao, L., Qu, X., You, Z., 2020a. Advances on molecular simulation technique in asphalt mixture. J. Traffic Transport. Eng. 20, 1–14, 02.
Wang, H., Ma, Z., Chen, X., Mohd Hasan, M.R., 2020b. Preparation process of bio-oil

and bio-asphalt, their performance, and the application of bio-asphalt: a comprehensive review. J. Traffic Transp. Eng. (Engl. Ed.) 7 (2), 137–151.
Wen, H., Bhusal, S., Wen, B., 2012. Laboratory evaluation of waste cooking oil-based bioasphalt as an alternative binder for hot mix asphalt. J. Mater. Civ. Eng. 25 (10), 1432–1437.
Xiu, S., Rojanala, H.K., Shahbazi, A., Fini, E.H., Wang, L., 2012. Pyrolysis and combustion characteristics of Bio-oil from swine manure. J. Therm. Anal. Calorim. 107 (2), 823–829.
Xu, G., Wang, H., 2017. Molecular dynamics study of oxidative aging effect on asphalt binder properties. Fuel 188, 1–10.
Xu, G., Wang, H., Sun, W., 2018. Molecular dynamics study of rejuvenator effect on RAP binder: diffusion behavior and molecular structure. Construct. Build. Mater. 158.
Xu, G.J., Wang, H., 2018. Diffusion and interaction mechanism of rejuvenating agent with virgin and recycled asphalt binder: a molecular dynamics study. Mol. Simulat. 44 (17), 1433–1443.
Xu, M., Yi, J., Feng, D., Huang, Y., 2019. Diffusion characteristics of asphalt rejuvenators based on molecular dynamics simulation. Int. J. Pavement Eng. 20 (5), 615–627.
Yang, X., Dai, Q., You, Z., Wang, Z., 2015. Integrated experimental-numerical approach for estimating asphalt mixture induction healing level through discrete element modeling of a single-edge notched beam test. J. Mater. Civ. Eng. 27 (9), 04014259.04014251-04014259.04014259.
Yao, H., Dai, Q., You, Z., Zhang, J., Lv, S., Xiao, X., 2019. Evaluation of contact angle between asphalt binders and aggregates using Molecular Dynamics (MD) method. Construct. Build. Mater. 212, 727–736.
You, L., Spyriouni, T., Dai, Q., You, Z., Khanal, A., 2020. Experimental and molecular dynamics simulation study on thermal, transport, and rheological properties of asphalt. Construct. Build. Mater. 265, 120358.
Zadshir, M., Hosseinnezhad, S., Ortega, R., Chen, F., Hochstein, D., Xie, J., Yin, H., Parast, M.M., Fini, E.H., 2018a. Application of a biomodifier as fog sealants to delay ultraviolet aging of bituminous materials. J. Mater. Civ. Eng. 30 (12), 04018310.
Zadshir, M., Oldham, D.J., Hosseinnezhad, S., Fini, E.H., 2018b. Investigating bio-rejuvenation mechanisms in asphalt binder via laboratory experiments and molecular dynamics simulation. Construct. Build. Mater. 190, 392–402.
Zargar, M., Ahmadinia, E., Asli, H., Karim, M.R., 2012. Investigation of the possibility of using waste cooking oil as a rejuvenating agent for aged bitumen. J. Hazard Mater. 233–234, 254–258.
Zhang, L., Greenfield, M.L., 2007a. Analyzing properties of model asphalts using molecular simulation. Energy Fuels 21 (3), 1712–1716.
Zhang, L., Greenfield, M.L., 2007b. Molecular orientation in model asphalts using molecular simulation. Energy Fuels 21 (2), 1102–1111.
Zhang, R., You, Z., Wang, H., Chen, X., Si, C., Peng, C., 2018. Using bio-based rejuvenator derived from waste wood to recycle old asphalt. Construct. Build. Mater. 189, 568–575.
Zhu, J., Zhou, C., 2019. Rationality evaluation index of asphalt molecular model. Mater. Res. Express 6 (11), 115110.